J. Fluid Mech. (1978), *vol.* 87, *part* 1, *pp.* 17–31
Printed in Great Britain

Interpretation of three-soliton interactions in terms of resonant triads

By D. ANKER AND N. C. FREEMAN
School of Mathematics, University of Newcastle upon Tyne, England

(Received 12 September 1977)

The three-soliton solution of the two-dimensional Korteweg–de Vries equation is analysed to show that the structure of the interaction can be represented in terms of the motion of two-soliton resonant interactions (*resonant triads*) as described by Miles (1977). The schematic development of the interaction with time is obtained and shown to approximate closely to computer calculations of the analytic solution. Similar results follow for interactions of more solitons and other equations.

1. Introduction

The soliton solutions of a wide class of nonlinear equations have been extensively studied both analytically and numerically. More recently this work has been extended to motions in higher dimensions, where infinite skew solitons propagate at angles to the main propagation direction. In particular, a study of solitary-wave interactions in two dimensions has been made by Miles (1977). His remarkable discovery that, in the interaction of two solitons, the interaction region between the incident solitons and the centre-shifted† solitons after interaction is essentially itself a single soliton leads to a very simple conceptual picture (figure 1) of the interaction process. This interaction soliton is the *resonant* soliton associated with the two incident solitons. Thus if the incident solitons have wavenumbers $\boldsymbol{\kappa}_1$ and $\boldsymbol{\kappa}_2$ with frequencies ω_1 and ω_2, the resonant soliton has wavenumber $\boldsymbol{\kappa}_2 - \boldsymbol{\kappa}_1$ and frequency $\omega_2 - \omega_1$. In particular, since the dispersion relation for the two-dimensional Korteweg–de Vries equation is $\omega = \kappa^3 \cos^3 \psi + 3\kappa \sin^2 \psi$, where $\boldsymbol{\kappa} = (\kappa \cos \psi, \kappa \sin \psi)$, this requires

$$(\tan \psi_1 - \tan \psi_2)^2 = (\kappa_1 \cos \psi_1 - \kappa_2 \cos \psi_2)^2.$$

When this condition is satisfied, the centre shift of each soliton due to the collision becomes infinite and only the incident solitons and the resonant soliton remain to form a *triad* (figure 2). This special solution of the equations can also be viewed as a fundamental entity as was the soliton itself.

It is of some interest therefore to ask whether more complex interactions can be described in terms of *solitons* and *triads*. In this paper we shall seek to explain the interaction of three Korteweg–de Vries solitons in this way although it is clear that the principles can be extended to higher-order interactions. The main difficulty in such extensions is their practical description. For the case of three solitons, it is comparatively simple to move in a co-ordinate system fixed with regard to the motion

† 'Centre shift' is often referred to in the literature as 'phase shift'. Since for more complex solitons the amplitude and phase are necessary for their description such a terminology becomes inconvenient.

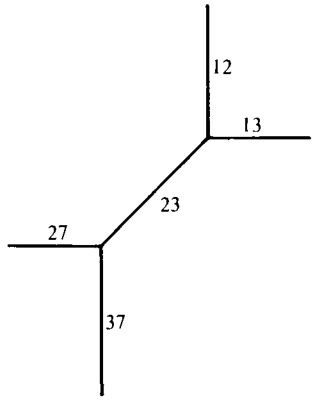

FIGURE 1. The two-soliton interaction of Miles showing two solitons (12) and (13) interacting to form centre-shifted solitons (37) and (27). The resonant soliton (23) is formed in the interaction. The plots are in terms of the phase variables η_1 and η_2.

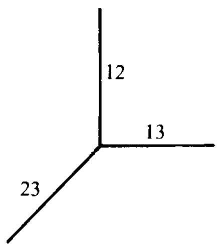

FIGURE 2. The triad (123) formed when the centre shift becomes infinite.

of two of the solitons and observe the third soliton sweeping over this, now static, configuration; such a procedure is not readily available for larger numbers of solitons. Analytically, the procedure is to group together the terms required to describe a soliton and a triad in the complete solution for a three-soliton interaction and assess their magnitude in various regions of the space and time domain. For the Korteweg–de Vries equation the complete solution may be viewed as a sum of eight terms any two of which form a soliton and any three of which a triad. Clearly, there are a large number of possibilities, viz. 28 solitons and 56 triads. Not all these possibilities can, of course, arise and the interest lies in choosing the sequence of these combinations which takes the configuration from one two-soliton interaction to another as the third soliton sweeps across. Each of the various triad intersections is associated with a particular set of three terms in the solution, and each can be labelled by three indices, just as each soliton can be labelled by two such indices. Such a description is very much an idealization since at each interaction point the condition for a resonant interaction is not met as the centre shift is not infinite. The centre shift is, however, determined by the parameters contained within the expression and by a suitable choice of such parameters it is possible numerically to approach the idealized situation. Computations have been made from the complete solution and the descriptive approach outlined above is vindicated in practice. Indeed, the availability of such a description leads to a close scrutiny of the computer records as the minute detail of the interaction is easily lost if large time steps are adopted for the computation.

While the description given here will be confined to soliton interactions associated with the Korteweg–de Vries equation, the similarity of the multi-soliton solutions of other equations of the class typified by this nonlinear partial differential equation shows that similar interactions occur with solutions of these equations also. The authors have been concerned with soliton solutions of the so-called Davey–Stewartson equation (Davey & Stewartson 1974; Davey & Freeman 1975; Anker & Freeman 1977). Here the equation for soliton amplitude is similar to that for the Korteweg–de Vries equation but the actual soliton is itself oscillatory and a phase angle is also necessary for its complete description. Details of the multi-soliton solution are given in the appendix for this case. In terms of amplitude alone it is shown to be almost identical to the Korteweg–de Vries result with a different definition for the parameters involved.

2. Solution for the interaction of three solitons

There are now many techniques available for obtaining the multi-soliton solution to the Korteweg–de Vries equation or, to be more accurate, its two-dimensional form as given by Kadomtsev & Petviashvili (1970). All such techniques rely on the equation having an underlying linear structure which enables the solutions to be constructed by inverse scattering theory. The direct approach used for many problems by Hirota, and for this problem by Satsuma (1976), is perhaps most convenient. In practice, the solution can most easily be written in terms of the second derivative of the logarithm of a determinant and it is this determinant which serves best to describe the interaction process. Few details of the solution procedure will be given here, but these may be found in the literature cited.

The two-dimensional Korteweg–de Vries equation may be written as

$$(u_t + 6uu_x + u_{xxx})_x + 3u_{yy} = 0, \tag{2.1}$$

where the coefficients have been chosen without loss of generality to make the analysis more tractable. The solutions may be visualized as waves of amplitude u moving in the x, y plane in time t. The suffixes denote partial derivatives.

It is of some interest to observe that the linearized form of (2.1) has plane-wave solutions whose phase variable $kx + my - \omega t$ satisfies the dispersion relation

$$\omega = (k^3 + 3m^2/k). \tag{2.2}$$

A more convenient way to parameterize this relation is to write $k = l+n$ and $m = n^2 - l^2$, whence

$$\omega = \frac{(l+n)^4 + 3(n^2-l^2)^2}{n+l} = 4(l^3+n^3). \tag{2.3}$$

This expression occurs naturally when the inverse scattering technique is employed (Zakharov & Shabat 1974).

The fundamental soliton solution of (2.1) is obtained as

$$u = \tfrac{1}{2}k^2 \operatorname{sech}^2 \tfrac{1}{2}(kx + my - \omega t) \tag{2.4}$$

with dispersion relation (2.2). With the above parameterization this becomes

$$u = \tfrac{1}{2}(l+n)^2 \operatorname{sech} \tfrac{1}{2}\eta = 2\,\partial^2[\log(1+e^{-\eta})]/\partial x^2, \tag{2.5}$$

where $\eta = -[(l+n)x + (n^2-l^2)y - 4(l^3+n^3)t]$.

Following Satsuma (1976), the three-soliton solution may now be computed in terms of the determinant Δ as

$$u = 2\,\partial^2(\log\Delta)/\partial x^2, \tag{2.6}$$

where

$$\Delta = \left|\delta_{ij} + \frac{A_i}{l_i+n_j}\exp\left[(l_i+n_j)\,x + (n_i^2-l_i^2)\,y - 4(l_i^3+n_i^3)\,t\right]\right|, \tag{2.7}$$

in which $i,j = 1,2,3$ and the A_i are constants. It will be observed that any exponential factor in Δ the argument of which is constant or linear in x does not contribute to u.

Expanding the determinant gives†

$$\begin{aligned}\Delta = \underset{(1)}{1} &+ \underset{(2)}{\exp(-\eta_1)} + \underset{(3)}{\exp(-\eta_2)} + \underset{(4)}{a\exp(-\eta_3)} + \underset{(5)}{a\epsilon_1\exp\{-(\eta_2+\eta_3)\}}\\ &+ \underset{(6)}{a\epsilon_2\exp\{-(\eta_1+\eta_3)\}} + \underset{(7)}{\epsilon_3\exp\{-(\eta_1+\eta_2)\}} + \underset{(8)}{a\epsilon_1\epsilon_2\epsilon_3\exp\{-(\eta_1+\eta_2+\eta_3)\}},\end{aligned} \tag{2.8}$$

with

$$\eta_i = -\left[(l_i+n_i)\,x + (n_i^2-l_i^2)\,y - 4(l_i^3+n_i^3)\,t\right] + \log\left[A_i/(l_i+n_i)\right] \quad (i = 1,2),$$

$$\eta_3 = \alpha\eta_1 + \beta\eta_2,$$

$$\epsilon_1 = (l_2-l_3)\,(n_2-n_3)/(l_2+n_3)\,(l_3+n_2), \text{ etc., by cyclic permutation,}$$

$$a = \left(\frac{A_3}{l_3+n_3}\right)\left(\frac{A_1}{l_1+n_1}\right)^{-\alpha}\left(\frac{A_2}{l_2+n_2}\right)^{-\beta}\exp\{-[(l_3^3+n_3^3)-\alpha(l_1^3+n_1^3)-\beta(l_2^3+n_2^3)]\,t\},$$

and

$$\alpha = \left(\frac{l_3+n_3}{l_1+n_1}\right)\left(\frac{l_2-l_3+n_3-n_2}{l_2-l_1+n_1-n_2}\right), \quad \beta = \left(\frac{l_3+n_3}{l_2+n_2}\right)\left(\frac{l_1-l_3+n_3-n_1}{l_1-l_2+n_2-n_1}\right).$$

The nomenclature is chosen in this way so that the motion of the solitons may be considered in a frame of reference in which η_1 and η_2 are fixed with the only time variation occurring in a. In fact we see that, depending on the sign of the coefficient of t in a, the coefficient a will range from 0 to ∞ or ∞ to 0. For $a = 0$,

$$\Delta = \underset{(1)}{1} + \underset{(2)}{\exp(-\eta_1)} + \underset{(3)}{\exp(-\eta_2)} + \underset{(7)}{\epsilon_3\exp\{-(\eta_1+\eta_2)\}} \tag{2.9}$$

represents the interaction of two solitons (12) and (13) centred on $\eta_1 = 0$ and $\eta_2 = 0$ respectively. Henceforth the solitons will be designated by number pairs giving their origin in the numbered terms of expression (2.8).

For $a \to \infty$, (2.8) becomes

$$\Delta \sim \underset{(4)}{1} + \underset{(5)}{\epsilon_1\exp(-\eta_2)} + \underset{(6)}{\epsilon_2\exp(-\eta_1)} + \underset{(8)}{\epsilon_1\epsilon_2\epsilon_3\exp\{-(\eta_1+\eta_2)\}}, \tag{2.10}$$

ignoring the factor $a\exp(-\eta_3)$, which does not contribute to u.

This represents the interaction of two solitons (45) and (46) centred on $\eta_1 = -\delta_2$ and $\eta_2 = -\delta_1$ respectively, where $\delta_i = \log\epsilon_i^{-1}$. The effect, therefore, of the interaction with the third soliton with phase variable η_3 is to change the interaction from one two-soliton interaction to the other. Thus assuming that the coefficient of t in a is positive, we begin with a picture (figure 1) for $t = -\infty$ or $a = 0$, with interaction of two solitons (12) and (13) centred on $\eta_1 = 0$ and $\eta_2 = 0$. Schematically, as has been observed by

† The terms have been numbered to facilitate the description of the interaction later.

Miles (1977), this results in two centre-shifted solitons (37) and (27) after interaction with centres on $\eta_1 = -\delta_3$ and $\eta_2 = -\delta_3$ and a resonant soliton essentially joining the intersection of these two sets along $\eta_1 = \eta_2$. The resonant soliton (23) is obtained in its entirety only when $\epsilon_3 \to 0$ or $n_1 \to n_2$ and it is then described by

$$\Delta_{23} \sim 1 + \exp\{-(\eta_1 - \eta_2)\}.$$

After the interaction with the third soliton is complete ($t = \infty$ or $a = \infty$), the picture is again that shown in figure 1 when, according to (2.10), the pre-interaction solitons (46) and (45) are centred on $\eta_1 = -\delta_2$ and $\eta_2 = -\delta_1$ and the post-interaction solitons (58) and (68) on $\eta_1 = -(\delta_2 + \delta_3)$ and $\eta_2 = -(\delta_1 + \delta_3)$. The resonant soliton (56) now lies along the line $\eta_1 - \eta_2 = -\delta_2 + \delta_1$. The whole picture has thus been translated a distance δ_2 in the η_1 direction and δ_1 in the η_2 direction.

The following question now arises: what happens between these two limits? In the next section, a qualitative picture of the interaction will be constructed.

3. Solutions and triads

The asymptotic field associated with the determinant Δ may be calculated once α and β are known. We shall assume for convenience that $\alpha, \beta, \delta_1, \delta_2, \delta_3 > 0$. The far-field solution may be obtained as $\eta_1, \eta_2 \to \pm\infty$ and comprises the following:

(i) Soliton (12) with $\Delta_{12} = 1 + \exp(-\eta_1)$, $\eta_1 > 0$, where the numbers refer to the terms of (2.8). A soliton centred on $\eta_1 = 0$.

(ii) Soliton (13) with $\Delta_{13} = 1 + \exp(-\eta_2)$, $\eta_2 > 0$, and centred on $\eta_2 = 0$.

(iii) Soliton (58) with $\Delta_{58} = a\epsilon_1 \exp\{-(\alpha\eta_1 + (\beta+1)\eta_2)\}[1 + \epsilon_2\epsilon_3 \exp(-\eta_1)]$, $\eta_1 < 0$, $\eta_2 < 0$. A soliton centred on $\eta_1 = -(\delta_2 + \delta_3)$.

(iv) Soliton (68) with $\Delta_{68} = a\epsilon_2 \exp\{-[(\alpha+1)\eta_1 + \beta\eta_2]\}[1 + \epsilon_1\epsilon_3 \exp(-\eta_2)]$, $\eta_1 < 0$, $\eta_2 < 0$. A soliton centred on $\eta_2 = -(\delta_1 + \delta_3)$.

(v) Soliton (26) with $\Delta_{26} = \exp(-\eta_1) + a\epsilon_2 \exp\{-[(\alpha+1)\eta_1 + \beta\eta_2]\}$, $\eta_1 < 0, \eta_2 > 0$. A soliton centred on $\alpha\eta_1 + \beta\eta_2 = -(A + \delta_2)$, where $A = \log a^{-1}$ (assumed positive).

(vi) Soliton (35) with $\Delta_{35} = \exp(-\eta_2) + a\epsilon_1 \exp\{-[\alpha\eta_1 + (\beta+1)\eta_2]\}$, $\eta_1 > 0, \eta_2 < 0$. A soliton centred on $\alpha\eta_1 + \beta\eta_2 = -(A + \delta_1)$.

A typical configuration is shown in figures 3 and 4. Solitons (12), (13) and (26) are obviously centre-shifted solitons (58), (68) and (35) respectively. In the case $\delta_1 = \delta_2$ solitons (26) and (35) are the asymptotic arms of the third soliton sweeping across the interacting pair (12) and (13). Solitons (58) and (68) are the centre-shifted solitons of the final two-soliton interactions referred to in § 2. For $\delta_1 \neq \delta_2$, the solution (2.8) allows a more general description in which the third soliton has different centre shifts at positive and negative infinity.

Now, prior to the third soliton sweeping across, (12) and (13) interact to give the centre-shifted solitons (37) and (27) respectively, and the resonant soliton (23) as discussed in § 2. It is therefore the interaction of the third soliton with this configuration which immediately concerns us. Soliton (26) will interact with (27) to form a resonant soliton (67) which combines with (26) and (27) to form the triad (267). The soliton (67) has the determinant

$$\Delta_{67} = \epsilon_3 \exp\{-(\eta_1 + \eta_2)\}\left(1 + \frac{a\epsilon_2}{\epsilon_3}\exp\{-[\alpha\eta_1 + (\beta-1)\eta_2]\}\right) \tag{3.1}$$

and thus is centred along

$$\alpha\eta_1 + (\beta - 1)\eta_2 = -(A + \delta_2) + \delta_3. \tag{3.2}$$

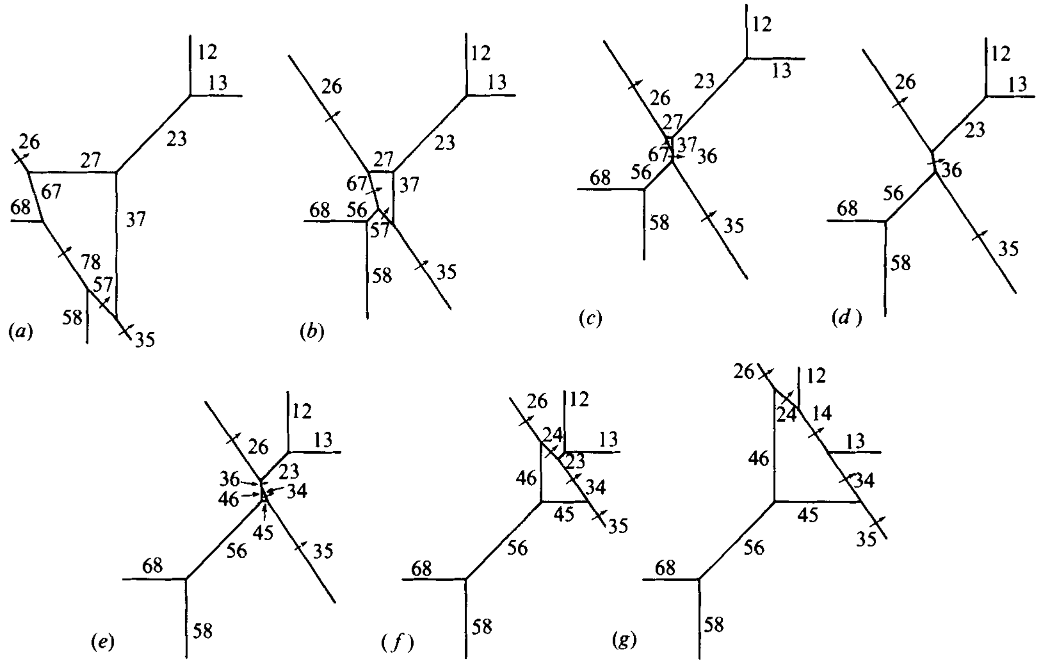

Figure 3. The sequence of events in the three-soliton interaction for $\delta_3 > \delta_1, \delta_2$ ($\delta_1 = 2$, $\delta_2 = 1$, $\delta_3 = 3$, $\alpha = 3$, $\beta = 2$). The plots are in terms of the phase variables η_1 and η_2.

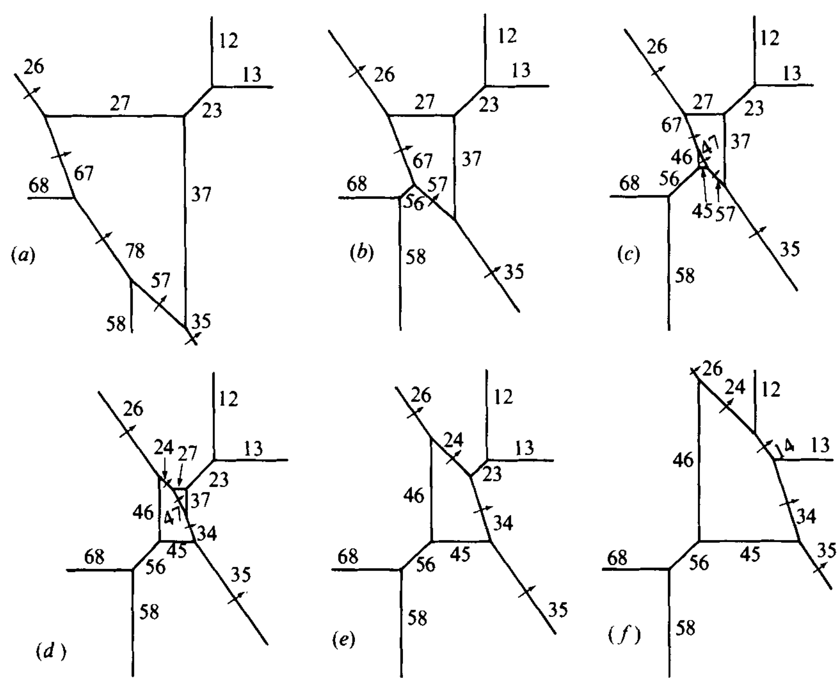

Figure 4. The three-soliton interaction for $\delta_3 < \delta_1, \delta_2$ ($\delta_1 = 3$, $\delta_2 = 2$, $\delta_3 = 1$, $\alpha = 3$, $\beta = 2$). The plots are in terms of the phase variables η_1 and η_2.

This soliton will interact with (68) to form a resonant soliton (78) with determinant

$$\Delta_{78} = \epsilon_3 \exp\{-(\eta_1+\eta_2)\}[1+a\epsilon_1\epsilon_2\exp\{-(\alpha\eta_1+\beta\eta_2)\}], \tag{3.3}$$

which is the phase-shifted third soliton

$$\alpha\eta_1+\beta\eta_2 = -(A+\delta_1+\delta_2). \tag{3.4}$$

These three solitons form the triad (678). Again, the soliton (78) interacts with the solition (58) to produce the resonant soliton (57) with determinant

$$\Delta_{57} = \epsilon_3 \exp\{-(\eta_1+\eta_2)\}\left(1+\frac{a\epsilon_1}{\epsilon_3}\exp\{-[(\alpha-1)\eta_1+\beta\eta_2]\}\right), \tag{3.5}$$

which is centred on $$(\alpha-1)\eta_1+\beta\eta_2 = -(A+\delta_1)+\delta_3. \tag{3.6}$$

These three solitons comprise the triad (578).

In turn the soliton (57) interacts with the soliton (35) to form the soliton (37), which brings us full circle, and the picture is complete as shown in figures 3(*a*) and 4(*a*). The only portions of the picture which are moving in this co-ordinate system are (26), (67), (78), (57) and (35).

As the motion proceeds soliton (78) reduces in length until, when it disappears, solitons (58) and (68) interact to form the resonant triad (568) and the resonant soliton (56) centred on $\eta_1-\eta_2 = -\delta_2+\delta_1$. This soliton is also resonant with the pair (67) and (57) (figures 3*b*, 4*b*). The further development now depends on the respective sizes of δ_3 and δ_1 and δ_2. The case $\delta_3 > \delta_1, \delta_2$ is depicted in figure 3 and $\delta_3 < \delta_1, \delta_2$ in figure 4. In the former case the triad (237) disappears before the triad (456) appears, in the latter the reverse occurs.

Following the first case, solitons (67) and (57) move across until the triad (567) interacts with the soliton (37). Solitons (67) and (37) then form the resonant triad (367) with resonant soliton (36). This soliton together with (56) and (35) forms a further triad. This configuration is shown in figure 3(*c*). Eventually the triangle diminishes to nothing as soliton (67) interacts with triad (237) and the arrangement becomes similar to that just described with a resonant triad (236) as shown in figure 3(*d*). The motion proceeds until the arms of the final soliton pair (46) and (45) appear (figure 3*e*); these resonate with (36) and (35) respectively to form a common soliton (34). This further develops until (26) and (46) resonate to form (24), which forms a triad with (23) and (34) (figure 3*f*). Finally, (24) and (34) interact with (12) and (13) respectively (figure 3*g*), to form the triads (124) and (134) with the common soliton (14). The original soliton pair interaction has now been moved laterally and longitudinally and the picture is the reflexion of figure 3(*a*).

In the second case, following figure 4(*b*), the development is somewhat different since solitons (45) and (46) appear first (figure 4*c*) and form the resonant triads (467) and (457) with common soliton (47). Now triads (467) and (237) both occur in the same picture. This picture is essentially reflected to form figure 4(*d*) later. Then the triad (237) disappears and solitons (24) and (34) interact directly with (23) in the triad (234) (figure 4*e*).

Finally, the reflexion of figure 4(*a*) is established (figure 4*f*) with the interaction of (24) and (34) with (12) and (13) respectively as before.

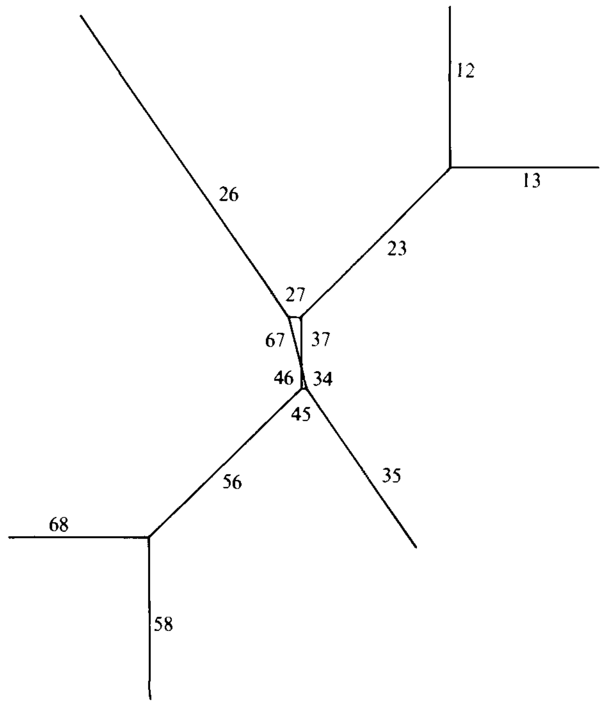

FIGURE 5. The case $\delta_1 = 3$, $\delta_3 = \delta_2 = 2$, $\alpha = 3$, $\beta = 2$.

Figures 3 and 4 thus indicate schematically the development of the three-soliton interaction. Since the triad interactions are incomplete for finite values of the parameters δ_1, δ_2 and δ_3, this description necessarily represents an idealization of the true interaction. Calculations have been undertaken on a computer to construct the true picture and are shown in figure 6 for the case corresponding to figure 4. It is clear that the idealized picture forms a good representation of the true picture when the values of the parameters δ_1, δ_2 and δ_3 are sufficiently large and the resonant solitons are large enough. The computer plots indicate the maxima of the function u in the field.

4. Computer solutions

To verify the procedure for the calculation of multi-soliton interactions discussed in § 3 it was decided to calculate the form of the amplitude u from (2.8) as a function of time in a particular case.

In order to make the comparison practical it was important to choose the values of l_i and n_i to give reasonable centre shifts as well as significant lengths of unmutilated soliton in the interaction. To do this it was necessary that the conditions were made close to resonance by choosing $n_1 \approx n_2 \approx n_3$ for a three-soliton interaction. Unfortunately, this limit leads to conditions very close to a degeneracy of the solution and the situations which arise are slightly different to those already encountered in § 3. Before discussing the solutions in detail therefore, it will be necessary to digress and study the nature of this difference.

Since the relative displacements of the solitons are associated with the quantities

l_1	l_2	l_3	n_1	n_2	n_3	δ_1	δ_2	δ_3	α	β
$-2{\cdot}01$	$3{\cdot}99$	$1{\cdot}99$	$3{\cdot}01-10^{-11}$	$3{\cdot}01+10^{-15}$	$3{\cdot}01$	$37{\cdot}4$	$25{\cdot}6$	$25{\cdot}5$	$1{\cdot}67$	$0{\cdot}476$

TABLE 1

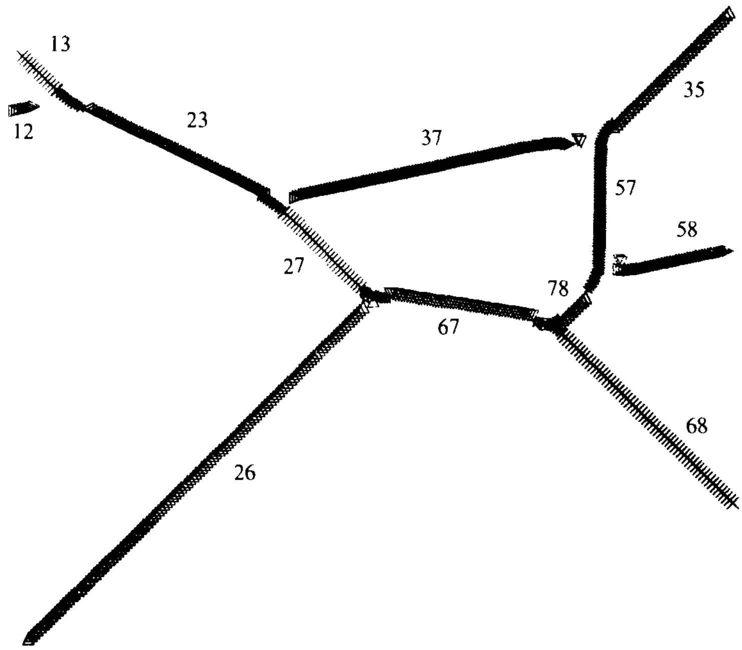

FIGURE 6(*a*). For legend see p. 29.

$\delta_i = \log \epsilon_i^{-1}$, it will be realized that, from the definition of ϵ_i, the value of δ_i will be determined numerically by the order of magnitude of ϵ_i or $n_j - n_k$ ($j \neq k \neq i$). Now, if the order of magnitude of $n_1 - n_3$ is significantly larger than the order of magnitude of $n_2 - n_3$, as will be necessary if a sufficient difference in the centre shifts is required, then $n_1 - n_3$ has an order of magnitude commensurate with $n_1 - n_2$. Thus $\delta_2 \approx \delta_3$. This implies the near alignment of solitons (37) and (46) in figures 3 and 4, for example. Hence figures 3 (*c*), 3(*d*), 4(*c*) and 4(*d*) become extremely distorted. Indeed if we consider the limiting situation when $\delta_2 = \delta_3$ as shown in figure 5, the situation approximates closely to the occurrence of a tetrad configuration formed by solitons (67), (37), (46) and (34).

The values of the parameters chosen for the computer solutions are shown in table 1. It will be observed that δ_1 and δ_2 are greater than δ_3 so that the situation corresponds to the soliton orientations discussed in figure 4 and δ_2 is very close to δ_3 as suggested earlier. A further slight difference is that $\beta < 1$, which introduces a sequence between figures 4 (*b*) and (*e*) similar to that encountered in figure 3 between figures 3 (*b*) and (*e*). The parameters chosen give significant angular differences in the directions of the solitons when plotted in the physical (x, y) plane and are preferable to those used in figures 3 and 4 for such plots. The computer results are shown in figures 6 (*a*)–(*e*), where the physical (x, y) orientation is used.

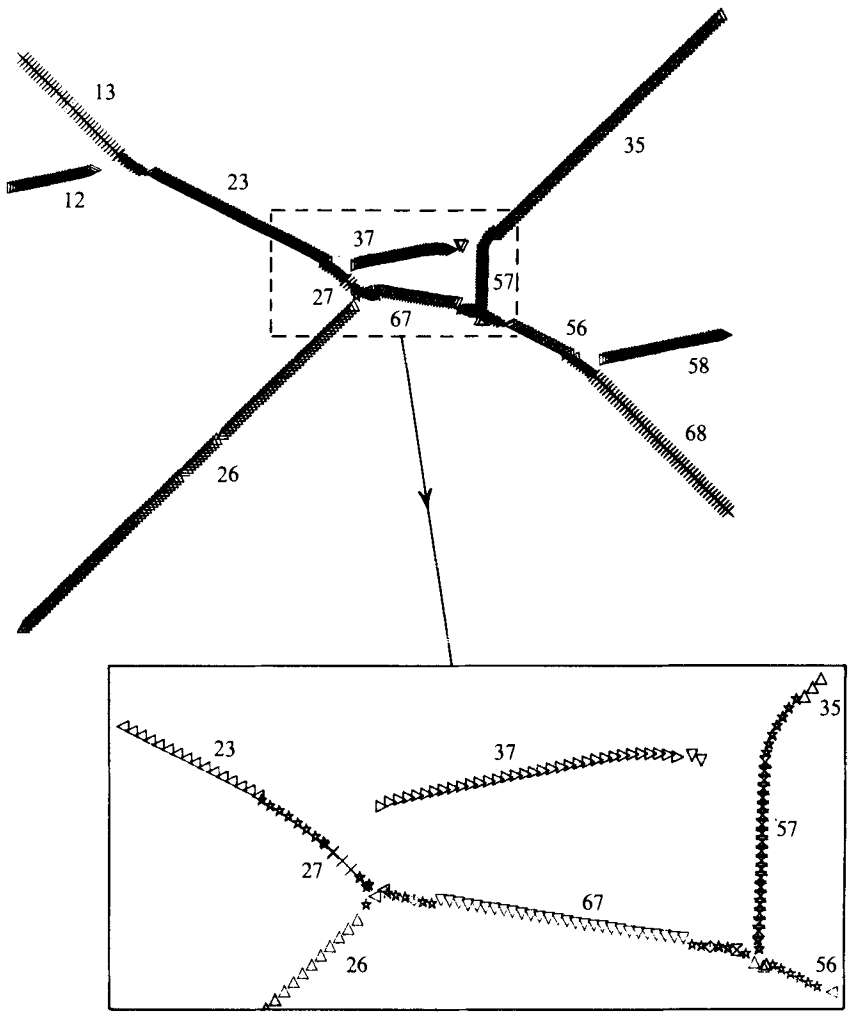

FIGURE 6(b). For legend see p. 29.

The technique employed for displaying the solitons was to choose symbols for the maxima of each soliton expected to appear in the interaction and instruct the computer to plot these maxima of the amplitude as calculated from (2.8). The amplitudes of these solitons are given in table 2 together with the symbols chosen. In practice, it was necessary to specify a range of values about these maxima for each symbol. The tolerance on these maxima was chosen to be half the minimum difference between the maxima of the solitons considered, namely 0·375. A tighter tolerance might perhaps be more desirable, but would have meant shorter solitons, which would have been more difficult to recognize. Any values which lay outside these ranges were plotted as a star. The array of amplitudes calculated over the whole x, y plane was scanned in both the x and the y direction for maximum values and these were plotted with the appropriate symbol. Such a scheme has its drawbacks since it is obviously possible to obtain maxima associated with individual solitons within the complex interaction regions between solitons. Thus spurious points not associated with the solitons themselves may be

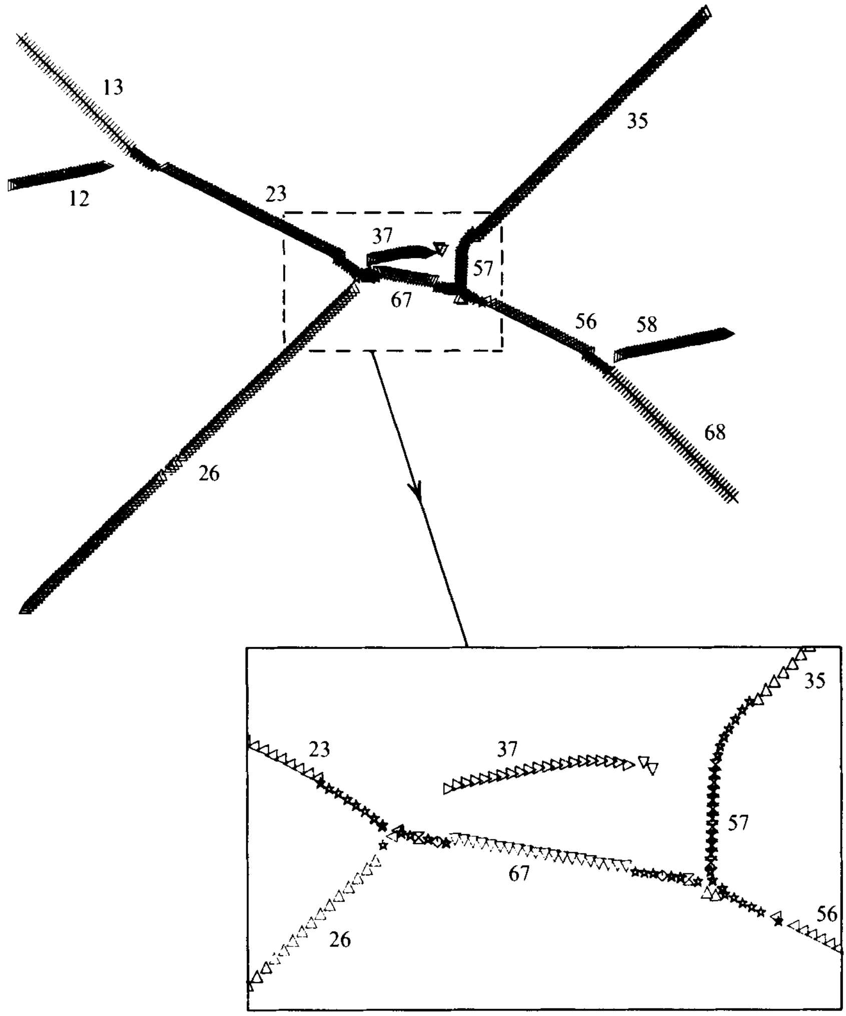

FIGURE 6(c). For legend see p. 29.

Symbol	Amplitude	Soliton(s)
▷	0·25	(12), (37), (46), (58), (36)
▽	1·00	(34, (67)
◇	2·25	(47)
⧗	4·00	(24), (57)
△	6·25	(14), (26), (35), (78)
◁	9·00	(23), (56)
×	12·25	(13), (27), (45), (68)
*	Denotes values outside a range of 0·375 either side of these values.	

TABLE 2

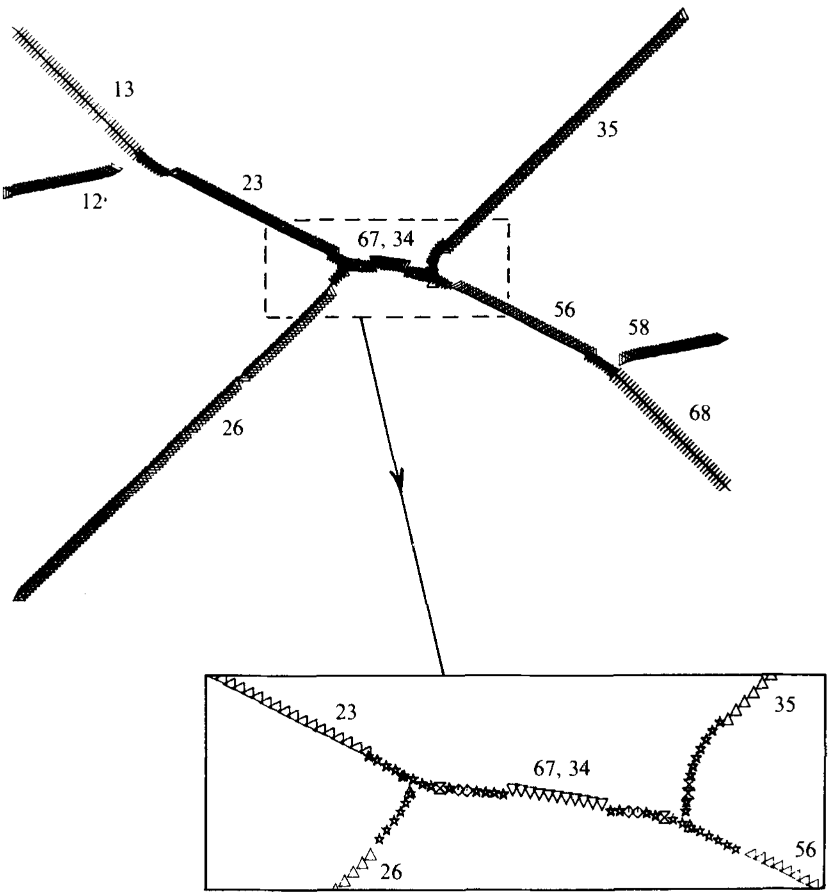

FIGURE 6(*d*). For legend see p. 29.

plotted. However, the system has the advantage that it is automatic and does not require any preconceived ideas about the form the interaction will take. The sequence of figures 6(*a*)–(*e*) indicates that the predicted development is closely followed. The corresponding solitons have been labelled with two figures as in figure 4. Figure 6(*a*) has the pentagonal form associated with figure 4(*a*), while the quadrilateral form of figure 6(*b*) corresponds to figure 4(*b*). Figures 6(*c*)–(*e*) are associated with the development depicted in figure 5 and, since $\beta < 1$, follow a similar development to figures 3(*c*) and (*d*) as mentioned above. It will, however, be observed that the solitons (34) and (67) tend to dominate the soliton (36), which is expected to occur in figures 6(*c*)–(*e*). This is mainly due to δ_2 being close to δ_3 and consequently figure 3(*c*) not occurring. The further development in time corresponds to figures 4(*e*) and (*f*), but since the computer plots associated with these are similar to figures 6(*a*) and (*b*) they are not given.

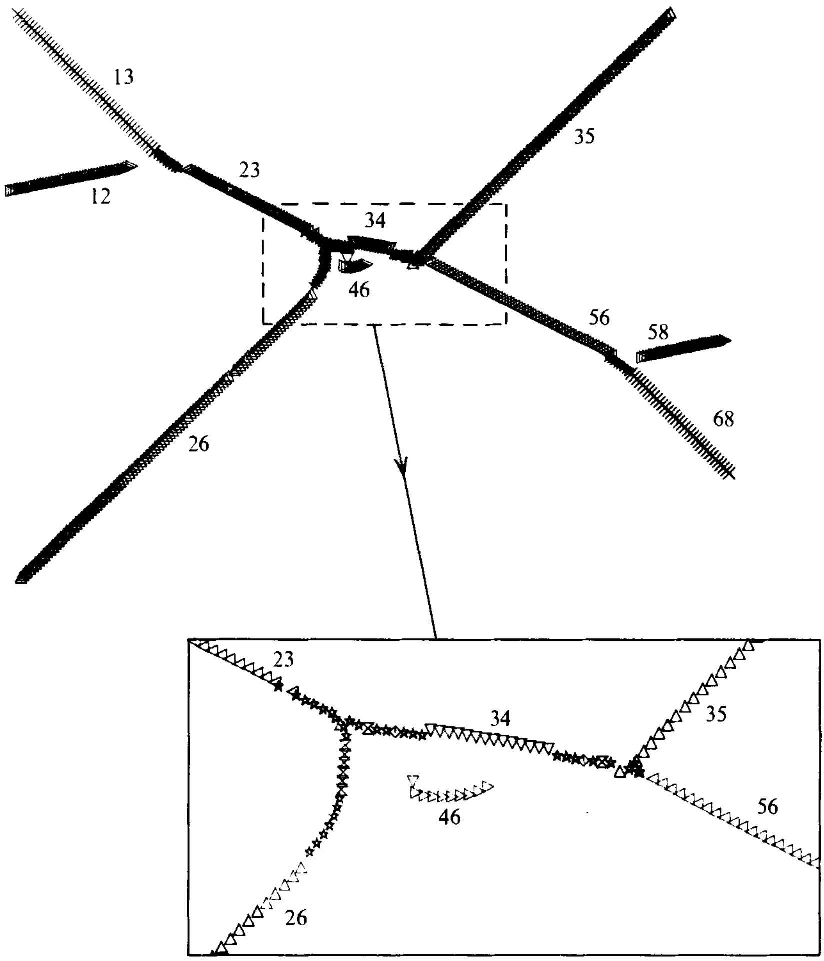

FIGURE 6. Computer plots of the three-soliton interaction for $\delta_3 < \delta_1, \delta_2$. Physical co-ordinates (x, y) are used. (a) $t = -\frac{1}{4}$, (b) $t = \frac{3}{8}$, (c) $t = \frac{1}{2}$, (d) $t = \frac{5}{8}$, (e) $t = \frac{3}{4}$.

5. Conclusion

The Miles resonance phenomenon has been shown to be a characteristic feature of soliton interaction when three solitons are considered. It seems clear that it will also permit an understanding of interactions involving a larger number of solitons. To do this, it becomes necessary to study the details of the algebra of the interaction process as a representation of the motion of the solitons in which they are denoted by couplets (ij) and triplets (ijk). It is obvious that instantaneously more than three solitons can come together, but in figures 3 and 4 this configuration does not persist. However, in the case $\delta_1 = \delta_2$ the figures become symmetrical about the (23), (56) line and figure 3 (*d*) would indicate that a tetrad is possible. It seems reasonable to suppose that with suitable values of the parameters other, more exotic configurations might appear. To describe such interactions will prove extremely complicated, but the beauty of the development described above might stimulate other workers to seek a more complete description of this fascinating phenomenon.

The authors are grateful to Professor A. C. Newell and Dr R. S. Johnson for many helpful discussions. One of us (D. A.) was in receipt of an S.R.C. Research Studentship during the period of this research.

Appendix. The n-soliton solution for the Davey–Stewartson equation

The basic determinantal solution for the multi-soliton solution of the Davey–Stewartson equation was given in Anker & Freeman (1977). Owing to the more complex nature of the fundamental soliton both the phase and the amplitude are required for a full description. This means that for an n-soliton solution a $2n \times 2n$ determinant is necessary to describe the amplitude variation. This can be written as the determinant of a partitioned matrix as follows:

$$\Delta = \left|\begin{array}{c|c} \delta_{ij} - A_i E_{ij} & -B_i^* E_{ij} \\ \hline -B_i E_{ij} & \delta_{ij} - A_i^* E_{ij} \end{array}\right|, \quad 1 \leqslant j \leqslant n, \quad 1 \leqslant i \leqslant n,$$

where $E_{ij} = \exp\{(l_i + n_j) x + m_i y - \gamma_i t\}/(l_i + n_j) = e_{ij}/(l_i + n_j)$ (say) and an asterisk denotes a complex conjugate.

A suitable parameterization of the dispersion relation gives

$$A_k = i a_k \exp\{\tfrac{1}{2} i(\theta_k + \phi_k)\}, \quad B_k = a_k \exp\{\tfrac{1}{2} i(\theta_k - \phi_k)\} \quad (a_k \text{ real}),$$

with $l_k = 2\sin\theta_k$, $n_k = 2\sin\theta_k$, $\beta m_k = 2\gamma(\cos\theta_k + \cos\phi_k)$ and $\alpha\gamma_k = 2(\cos 2\theta_k - \cos 2\phi_k)$.

Noting that $|A_k| = |B_k|$, multiplication of rows and columns by suitable factors then reduces Δ to

$$\left|\begin{array}{c|c} \delta_{ij} & 0 \\ \hline -\dfrac{B_i B_i^*}{A_j} E_{ij} & B_i^* \left[\dfrac{\delta_{ij}}{B_j^*} - \left(\dfrac{A_i^*}{B_j^*} + \dfrac{B_i}{A_j^*}\right) E_{ij}\right] \end{array}\right|$$

$$= |\delta_{ij} - (A_i^* + B_i B_j^*/A_j^*) E_{ij}|$$

$$= |\delta_{ij} + 2a_i e_{ij} \sec\tfrac{1}{2}(\theta_i - \phi_j)|$$

$$= 1 + \sum_{m=1}^{n} \sum_{i_m, j_m} |\sec\tfrac{1}{2}(\theta_{i_m} - \phi_{j_m})| \prod_{i_m} \tfrac{1}{2} a_{i_m} \exp(-\eta_{i_m}),$$

with $$\eta_k = -\left[2(\sin\theta_k + \sin\phi_k) x + \frac{2\gamma}{\beta}(\cos\theta_k + \cos\phi_k) y - \frac{2}{\alpha}(\cos 2\theta_k - \cos 2\phi_k) t\right],$$

where i_m and j_m denote the rows and columns of the matrices formed by taking the elements associated with all combinations of m main-diagonal elements.

In particular, for the case $n = 2$ we obtain

$$\begin{aligned}\Delta = {} & 1 + a_1 \sec\tfrac{1}{2}(\theta_1 - \phi_1) \exp(-\eta_1) + a_2 \sec\tfrac{1}{2}(\theta_2 - \phi_2) \exp(-\eta_2) \\ & + [\sec\tfrac{1}{2}(\theta_1 - \phi_1) \sec\tfrac{1}{2}(\theta_2 - \phi_2) - \sec\tfrac{1}{2}(\theta_1 - \phi_2) \sec\tfrac{1}{2}(\theta_2 - \phi_1)] a_1 a_2 \exp\{-(\eta_1 + \eta_2)\},\end{aligned}$$

a result similar to that for the Korteweg–de Vries soliton with a resonance condition of the form $\theta_1 = \theta_2$ or $\phi_1 = \phi_2$. A similar result also follows for the three-soliton case and hence the procedures used to describe the interaction in this paper can be used also in that case. This suggests that the procedures will be available for the whole class of equations solvable by inverse scattering theory in the manner of Zakharov & Shabat (1974) for their multi-soliton solutions.

REFERENCES

ANKER, D. & FREEMAN, N. C. 1978 *Proc. Roy. Soc.* A **360**, 1703.
DAVEY, A. & FREEMAN, N. C. 1975 *Proc. Roy. Soc.* A **344**, 427–433.
DAVEY, A. & STEWARTSON, K. 1974 *Proc. Roy. Soc.* A **338**, 101–110.
KADOMTSEV, B. B. & PETVIASHVILI, V. I. 1970 *Dokl. Akad. Nauk SSR* **192**, 753–756.
MILES, J. W. 1977 *J. Fluid Mech.* **79**, 171–179.
SATSUMA, J. 1976 *J. Phys. Soc. Japan* **40**, 286–290.
ZAKHAROV, V. E. & SHABAT, A. B. 1974 *Functional Anal. Appl.* **8**, 226–235.